Int. J. Heat Mass Transfer. Vol. 13, pp. 345–358. Pergamon Press 1970. Printed in Great Britain

RADIATIVE HEAT TRANSFER ANALYSIS FROM A HEATED AIRPORT RUNWAY TO FOG

GORDON L. SCOFIELD*

Mechanical and Aerospace Engineering Department, University of Missouri-Rolla, Rolla, Missouri 65401

and

TOM J. LOVE

School of Aerospace and Mechanical Engineering, University of Oklahoma, Norman, Oklahoma 73069

(*Received* 24 *October* 1968 *and in revised form* 7 *May* 1969)

Abstract—Radiative heat transfer between a plane source and an aerosol is investigated through the Monte Carlo method. Thermal energy is transferred from a long rectangular source to monodisperse natural fog models. The analysis is only for radiative transport and does not include convection which would be coupled in a complete analysis. Direct energy transfer to the droplets of the aerosol is investigated for values of extinction coefficient of 10 km^{-1} and 80 km^{-1}, absorption coefficient to extinction coefficient ratios of 0·4 and 0·5, and scattering functions of the strong forward and isotropic types. Monochromatic radiation at a wave length of 10 μ is used and multiple independent scattering is included. The numerical results are illustrated in a manner which expresses the spatial distribution of radiative interactions and exposes the implications of this mode of energy exchange as a means of fog dispersal over airport runways.

NOMENCLATURE

Probability distribution functions

F_y, y coordinate for point of source emission;

F_{η_E}, polar angle of source emission measured from a translated rectangular axis system;

F_{ψ_E}, azimuthal angle of source emission measured from a translated rectangular axis system;

F_s, free path length of energy bundle;

F_{abs}, discrete fraction of interactions that are absorptions;

F_{scat}, discrete fraction of interactions that are scatterings;

$F_{\eta_{(I)}}$, polar angle of isotropic scattering measured from a translated rectangular axis system;

$F_{\psi_{(I)}}$, azimuthal angle of isotropic scattering measured from a translated rectangular axis system;

$F_{\eta_{a(A)}}$, polar angle of anisotropic scattering measured from a translated–rotated rectangular scattering axis system;

$F_{\psi_{a(A)}}$, azimuthal angle of anisotropic scattering measured from a translated-rotated rectangular scattering axis system;

$F_{\eta_{a(F)}}$, polar angle of strong forward scattering model measured from a translated–rotated rectangular scattering axis system.

Other nomenclature

y, y coordinate of point of source emission (L);

w, half width of long rectangular source (L);

* Present address: Mechanical Engineering Department, Michigan Technological University, Houghton, Michigan 49931.

η, polar angle measured from translated rectangular axis system [rad];
ψ, azimuthal angle measured from translated rectangular axis system [rad];
s, energy bundle path length along direction of motion (L);
β_o, volume extinction coefficient or optical density (L^{-1});
M.F.P., mean free path of energy bundle (L);
abs/ext, ratio of absorption coefficient to extinction coefficient;
Ω, total solid angle [sr];
$\hat{I}_{(\eta_s)}$, normalized intensity distribution;
η_s, polar angle measured from translated–rotated rectangular scattering axis system [rad];
ψ_s, azimuthal angle measured from translated–rotated rectangular axis system [rad];
$d\omega$, differential solid angle [sr].

INTRODUCTION

THE DISPERSAL of fog from airport runways, in support of commercial airline operations, is increasingly attractive for economic reasons due to accretion in the number of flights and programmed future growth in payload per flight. While specialized fog seeding techniques are applicable to the dissipation of certain fog types, thermal dissipation continues to be of interest due to its applicability to all fog types. Thermal dissipation utilizing the radiative mode of heat transfer is inherently attractive because of its unique ability to transfer heat directly to fog droplets at some distance from the source [1].

A partial review of fog dispersal systems and fog characteristics should prove helpful in establishing a perspective for the material which follows. Thermal dissipation of fog over airport runways was effected during World War II for military aircraft operating in England. These systems, as well as others closely related to them, employed lines of open flame burners, oriented in an appropriate manner parallel to the runway, to transfer thermal energy to the surrounding fog. This type of system is often referred to as a FIDO (Fog Investigation and Dispersal Operation) system. Permanent or mobile systems of the FIDO type have supported commercial and/or military operations in the United States. Their operation has been satisfactory in a limited way; however, heavy fog or fog combined with a strong cross wind has not been satisfactorily dispersed [2].

While all types of fog are amenable to thermal dissipation in principle, other dispersion techniques have been found well suited to certain fog types. Fog can be classified, in an oversimplified way, as ice fog, cold fog or warm fog. Ice fog is an aerosol in which the particles are ice crystals and is found at very low temperatures, perhaps 30–50 degrees below zero Fahrenheit [3]. Thermal dissipation is the only technique currently applicable to this fog type. Cold fog is somewhat unique though not uncommon. This type of fog contains liquid droplets at a temperature below their freezing point and is sometimes called super-cooled fog. This unstable condition has led to successful dissipation of this particular fog type by seeding the fog bank from low flying aircraft or ground generators [1, 4]. A partial list of the seeding agents used might include dry ice, silver iodide and liquefied petroleum gas. These seeding agents produce ice crystals of sufficient size to separate from the fog under the influence of gravity. Warm fog is stable in that the liquid droplets exist above their freezing point temperature. Until recently the dissipation of this type of fog was dependent on thermal systems. Currently large scale experiments, which seed the warm fog with nuclei which cause preferential growth by absorbing water vapor from the air with subsequent fog droplet evaporation, show promise [5–7].

Because of their general applicability as well as their versatile adaptability to a variety of physical implementations, the thermal dissipation systems continue to be of interest. As mentioned earlier, the radiative mode of heat transfer allows heat to be transferred directly to fog

droplets located at some distance from the source. There are certain wavelength intervals which are transparent for the suspending medium, the atmosphere, but which act as "windows" through which heat can be transferred to the water droplets[8]. The numerical results of this paper are based on warm fog models. The radiant energy absorbed by a droplet is the mechanism by which evaporation, or thermal dissipation, of the fog takes place. The continuous absorption spectrum of the liquid water droplets is sympathetic to this "window" interval type of direct transfer. The coupled problem of the radiation energy at wavelengths outside the "window", which is absorbed by the water vapor and carbon dioxide in the atmosphere with subsequent temperature and relative humidity changes in the suspending medium, is not considered explicitly in this paper.

The preceding discussion of fog dispersal provides a practical background for the theoretical development described in this work. The problem defined and the analysis presented is only for the radiative transport, or the direct transfer of energy from the source to the fog droplets. A complete analysis of energy transfer would require the coupling of both radiative and convective transport. Convective heating, were it included, could be expected to assist in fog dissipation. In addition, the time dependent character of the physical and optical properties of the aerosol during dissipation would be essential to a complete analysis of the energy transport for any particular source–aerosol model. The analysis in this work does not purport to develop this transient aspect of the problem. The contribution intended is to provide a useful and practical analytical approach to the instantaneous rate of radiative heat transfer for a source–aerosol model having practical implications. Extension of the method to other source–aerosol models is possible.

PHYSICAL MODEL

In this paper the runway itself is heated to a moderate temperature, comparable to that which might exist on a desert air strip on a summer day, to act as the source of radiant energy. This large isothermal source at a moderate temperature represents a departure from previous work. Since a runway is very long compared to its width, it might be tempting to assume an infinite length. It can be shown that such an assumption is appropriate over most of the runway length. Infinite length, coupled with an isothermal runway, leads to a uniform rate of radiative exchange with longitudinal position. That is, any plane perpendicular to the longitudinal axis of the runway would exhibit the same radial distribution of radiative exchange as any other similar plane at some other longitudinal position. The previous arguments and assumptions do not eliminate the requirement that the three dimensional extent be used as the proper physical model; however, it does allow the three dimensional distribution of radiative exchange to be folded into a typical two dimensional radial plot. Figure 1 gives explicit form

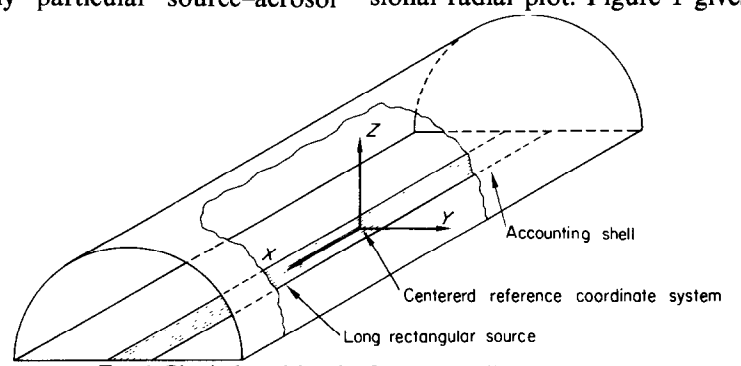

FIG. 1. Physical model and reference coordinate system for long rectangular source.

to the source geometry and the centered reference coordinate system. The Y–Z plane in this illustration will serve to establish the radial distribution of radiative exchange.

Since absorptions of radiative energy are related to the dissipation of fog by evaporation, the distribution of absorptions in the surrounding aerosol is requisite to the determination of local rates of dispersal. For this reason, the surrounding aerosol should be divided into two regions, one inside an accounting shell where practical contributions are made to fog dissipation, and one outside the accounting shell where it is assumed that practical contributions are negligible. The physical shape of this boundary condition is somewhat arbitrary. The half cylinder shown in Fig. 1 has been selected for this paper. For reasons which will be developed later in the paper, a subdivision of the space inside the accounting shell will be helpful to analysis. The particular subdivision selected for this work is shown in the positive quadrant of the Y–Z plane in Fig. 2. A matrix notation is used to note the ray number and radial increment of the subject subspace volume as indicated in Fig. 2.

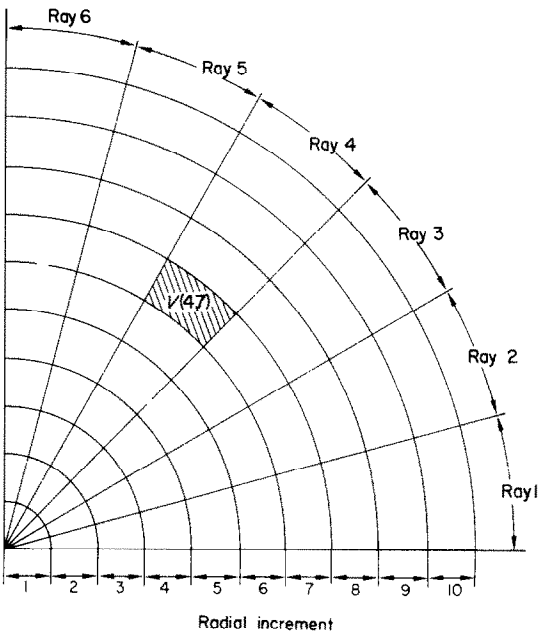

FIG. 2. Subdivision of accounting envelope cross section into sixty subspaces.

AEROSOL MODEL

A correlated set of physical and optical properties, consistent with those representative of natural fog, is essential to the structure of specific problems for numerical analysis. There can be no question that fog is a polydispersion and most investigators agree that it has a unimodal size distribution of droplets [9]. Due to the shape of the typical size distribution curve, it is impossible to have a common mean radius with which to express such parameters as droplet circumference, cross sectional area, and volume [10]. Because of analytical difficulties posed by polydispersions, monodispersions in which droplets are all of the same size have been used for many investigations, including this work. The droplet sizes chosen for the monodisperse fog models of this paper reflect the droplet sizes of greatest population in actual fog and thus should provide reasonable fog models. Reasonable limits of liquid water content and droplet number density are maintained on the basis of published empirical studies [1, 11].

Optical properties are a function of wavelength, droplet size, droplet number density and relative index of refraction. The optical properties of specific interest are the extinction coefficient, the ratio of absorption coefficient to extinction coefficient, and the angular distribution of scattered radiation. Since the "window" of direct heat transfer to the water droplets in the atmosphere extends from about 7·5 to 13·5 μ in wavelength, a monochromatic model at a wavelength of 10 μ is assumed to characterize the radiation throughout the "window" interval. Because the problem is thus converted to a quasi-monochromatic case, for convenience, the usual frequency or wavelength subscripts for optical properties will not be carried. Values of volume extinction coefficient were chosen to represent a wide range of expected visibility [12, 13]. The ratio of absorption coefficient to

extinction coefficient was established from published data on the complimentary parameter often called albedo [14, 15]. The scattered intensity distribution is available through published information based on the application of Mie theory or the collection of empirical data [14, 16]. The distribution of scattered intensity is similar for either approach and shows a very strong forward scattering tendency with a very weak back scattered component [14, 17]. A scattering distribution which is a reasonable model of this strong forward scattering tendency was chosen for this paper. In addition, the often used assumption of isotropic scattering is investigated for comparative purposes.

ANALYTICAL MODEL

The radiant energy streaming from the source will produce interactions, absorptions and multiple anisotropic or multiple isotropic scatterings, in the surrounding aerosol. In this work radiant energy is characterized by a large number of discrete energy bundles being released from the source to penetrate into the aerosol along paths governed by appropriate probability distributions. The Monte Carlo method makes it possible to synthesize a probable history for each energy bundle from source emission through a sequence of free paths and interactions until a history terminating event takes place. A large number of such histories is required to assure an accurate representation of the radiative transfer. In the example problem used in this paper only two events can cause the termination of a history, namely, an escape from the accounting shell or an absorption. Since an escape takes the bundle of energy to a spatial location where it is assumed that no practical contribution to the problem is possible, this type of termination is recorded as an escape and a new energy bundle history is initiated. The base plane, contiguous with the source, is considered an integral part of the accounting shell. When the terminating event is an absorption within the accounting shell, it is relevant to ask where the absorption with its transfer of energy took place. For absorption interactions within the accounting shell it would be possible to register individual coordinates for each such absorption. Meaningful evaluation of the spatial distribution of such absorptions would be difficult. For this reason, a finite subdivision of the accounting shell is indicated. While such subdivision is to some extent arbitrary, each subspace must be small enough to argue in favor of uniform properties and parameters within it but large enough to provide statistical information in which confidence is satisfactory.

The Monte Carlo method used to implement the appropriate statistical analytical model requires that each event in the history of a bundle of energy must have a known probability distribution function. This distribution function is a monotonic increasing function defined over the range of possible outcomes, discrete or continuous, of a given event and takes on all values from zero to unity [18]. By equating this distribution function to a large sequence of random numbers, uniformly distributed from 0 to 1, the appropriate frequency for each possible outcome of the event is generated. The digital computer is well suited to conduct experiments in which random numbers, uniformly distributed from 0 to 1, are equated to the probability distribution function, and, further, it can be programmed to provide efficiently an almost limitless supply of the requisite random numbers. While the random numbers produced in this manner are actually pseudo-random numbers, they will be called random numbers in this paper.

The distribution functions must be established for all events in a history, such as the point of emission, direction of emission, length of free path to the point of interaction, type of interaction, and continuing free paths between scattering interactions until a history terminating event takes place. In general, the distribution functions can be derived from known physical principles, either analytical or empirical in nature, or from carefully constructed hypotheses [19, 20]. The statistical model, and the sub-

sequent answers it produces, is no better than the distribution functions constructed and the convergence of the numerical results to stable event frequencies. Each problem will require some trial and error regarding the number of histories required to establish acceptable confidence in the statistical frequencies generated [21, 22].

Each history is started by the release of a bundle of energy from the source. The coordinates of the point of emission and the direction of the emission are the initial considerations for the history. The coordinates are a function of the shape of the source, in this paper a long rectangle, the type of coordinate system used to define the shape analytically, rectangular in this work, and the temperature distribution. The practical implications of fog dissipation suggest a probable goal of a black diffuse isothermal source. This particular temperature distribution means that each small area on the source will release the same number of bundles of energy as any other area of similar size at an arbitrary location on the source.

In the event that the rectangular source is very long compared to its width, the assumption of an infinite length can be made. By placing the origin of the rectangular coordinate system at the center of this source model, it is possible to take advantage of the symmetry that results. Under these circumstances it can be shown that a line source model extending from the center of the source to its edge along the positive extension of the Y axis (Fig. 1) is a satisfactory model. While emission must take place from an area, the line source model produces equivalent interaction distribution with a small saving in computer time. A line source model of this type would be satisfactory over most of the emitting length of a heated airport runway. The appropriate probability distribution function for such a model is given by

$$F_y = \frac{y}{w}, \tag{1}$$

where w represents one half the width of the runway and y is the coordinate of the point of emission, both dimensions being measured in a common system of units.

The direction of emission for a diffuse surface such as that assumed for this study follows the cosine law. The direction can be determined in spherical coordinates measured from a set of translated rectangular coordinates brought to the point of emission. The polar angle, η, is measured from the positive extension of the Z_t axis, while the azimuthal angle, ψ, is measured counterclockwise from the positive extension of the X_t axis. The t subscript indicates a translated rectangular coordinate system. The appropriate probability distribution functions for the selection of these two angles are

$$F_{\eta_E} = \cos^2 \eta, \tag{2}$$

and

$$F_{\psi_E} = \frac{\psi}{2\pi}, \tag{3}$$

where the angles are measured in radians.

Now that the point of emission and the direction of emission are known, it is necessary to determine the length of the free path that will be traveled in this direction before an interaction is encountered. Using the volume extinction coefficient at the quasi-monochromatic wavelength of 10 μ established for the example problem leads to a distribution function for free path length of

$$F_s = \exp(-\beta_o s), \tag{4}$$

where β_o is the volume extinction coefficient and s is the free path length in compatible units.

The mean free path (M.F.P.) of an energy bundle between emission and an interaction, or between interactions can be expressed as

$$\text{M.F.P.} = \frac{1}{\beta_o}. \tag{5}$$

At the end of each free path an interaction takes place and must be either a scattering or an absorption. Since extinction coefficient is the

sum of scattering coefficient and absorption coefficient, the sum of the ratios of absorption and scattering coefficients to extinction coefficient is unity. The individual ratios tell the proportion of extinction interactions that are absorptions or scatterings. If the ratio of absorption coefficient to extinction coefficient is called abs/ext, the appropriate distribution functions for this discrete choice can be written as the inequalities

$$0 \leqslant F_{\text{abs}} \leqslant \text{abs/ext}, \tag{6}$$

and

$$\text{abs/ext} < F_{\text{scat}} \leqslant 1. \tag{7}$$

Extinction as a result of absorption is characterized by an energy bundle being captured by a particle of the aerosol. The energy in the bundle that is captured is transformed into some form of internal energy for the particle. The history of the energy bundle is terminated at the point of absorption, the spatial location documented in terms of the subspace of the accounting envelope, see Fig. 2, within which it has occurred, and the statistical solution is continued by returning to the source to initiate the release of another energy bundle. In this work the aerosol is natural fog, and as a result, the internal energy transformation of the absorbed energy might result in a small portion of the droplet being evaporated. Experiments with a narrow beam of radiation, as compared to the field of radiation provided in this study, indicate the complexities of relating absorbed energy to droplet evaporation [23]. In this work it is assumed that all absorbed energy is converted to evaporation of the droplet. Thus, local absorption rate can be converted to local evaporation rate. Although this oversimplifies the actual phenomena, the results obtained will have a high degree of usefulness for comparative purposes. Experimental work with a field of radiation would be essential in order to produce more definitive results for inclusion in the analytical model of this paper.

In the event the interaction is determined to be a scattering, a rather more complicated analysis is required. Some background is in order as a starting point [24, 25]. Coherent scattering, the condition that the scattered and incident radiation are of the same wavelength, is assumed, and polarization effects are neglected due to their suppression by diffuse emission and multiple reflections. Since the droplets are separated by more than three radii, independent scattering is considered to exist although multiple independent scatterings for each bundle of energy are considered when appropriate.

The complexities of scattering analysis often lead to the simplifying assumption of isotropic scattering. The validity of this assumption is tested in the comparative numerical data of this paper. The appropriate distribution functions for the polar and azimuthal angles of the isotropically scattered energy bundle are

$$F_{\eta(I)} = -\tfrac{1}{2}\cos\eta + \tfrac{1}{2}, \tag{8}$$

and

$$F_{\psi(I)} = \frac{\psi}{2\pi}, \tag{9}$$

where η is the polar angle and ψ is the azimuthal angle, measured in radians as previously indicated from an appropriate translated rectangular system of axes with origin at the point of the scattering. The equally likely direction of scattered intensity for isotropic scattering allows the use of a translated axis system as the basis for analytical work.

Actually, the Eulerian approach, involving the incoming energy being coincident with the Z_s axis, with the incoming and outgoing energy being in the Z_s–Y_s plane, is the usual way of treating scattering phenomena. The s subscript refers to the translated and rotated scattering axis system. In the case of anisotropic scattering, such a translated–rotated axis system is required with subsequent transformation of spatial information back to the initial reference cartesian coordinate system, shown in Fig. 1. The distribution of scattered intensity for the anisotropic case can be obtained by application of Mie theory

or by appealing to empirical data where available. In either case the application of the Monte Carlo method is enhanced by the use of normalized intensity distribution. By definition, this distribution is such that

$$\frac{1}{4\pi}\int_{\Omega}\hat{I}(\eta_s)\,d\omega = 1, \tag{10}$$

where $\hat{I}(\eta_s)$ is the normalized intensity, $d\omega$ is the differential solid angle, and Ω indicates integration over all solid angles. Expansion of the differential solid angle in terms of the polar and azimuthal angles in the scattering coordinate system and separation of this integrand into the appropriate statistically independent probability distribution functions for these angles leads to

$$F_{\eta_s(A)} = \int_0^{\eta_s}\frac{\hat{I}(\eta_s)\sin\eta_s}{2}\,d\eta_s, \tag{11}$$

and

$$F_{\eta_s(A)} = \frac{\psi_s}{2\pi}, \tag{12}$$

where η_s is the scattering polar angle and ψ_s is the equally likely azimuthal angle, both measured in radians in the scattering coordinate system.

The preceding equation for the distribution of the polar scattering angle is not explicit in the form shown, and it is usually necessary to resort to some approximating device to evaluate the integral for increasing values of the polar angle. In this work the integrand was plotted and graphically integrated for increasing values of polar angle within its range. The resulting probability distribution curve can be fitted, within discrete ranges of the distribution function, with simple analytical expressions well adapted to the Monte Carlo method. The appropriate analytical expression from this sequence can be called up on the basis of the random number selected to characterize the distribution function.

Although the method just discussed was implemented for a number of example source–aerosol models, a somewhat simpler approach was found to produce comparable interaction distribution [26]. This approach features a simple exponential distribution function which is somewhat more strongly forward scattering but bears a close resemblence to the theoretical and empirical distribution functions for natural fog. The strong forward scattering distribution function for polar scattering angle is

$$F_{\eta_s(F)} = 1 - \exp\left(-\frac{13{\cdot}5\eta_s}{\pi}\right), \tag{13}$$

where η_s is the polar angle measured in radians from the positive extension of the Z_s axis in the scattering coordinate system.

The only remaining event that has not been discussed in some detail is that involving escape of the energy bundle from the accounting shell. The end of each free path connotes either a scattering, an absorption, or an escape. Since the end of each free path is the point of the next interaction, this point can be determined in the appropriate coordinate system and then transformed into coordinates of the fixed reference coordinate system centered in the source as shown in Fig. 1. Since the location of the boundary of the accounting shell is known with reference to this same coordinate system, the test for an escape is straight forward.

NUMERICAL RESULTS

The digital computer is ideally suited to make the simple but extensive series of calculations and decisions required to obtain results having statistical meaning. In order to give numerical structure to the example problem, various dimensions and properties must be assigned to the source–aerosol model.

The isothermal source is assumed black and diffuse at a temperature of 600°R or 333°K. It is 50 m wide and 2500 m long. The radius of the accounting shell is 125 m. The portion of the total emitted energy that streams through the wavelength interval between 7·5 and 13·5

μ is approximately 40 per cent. The highest efficiency, about 41 per cent, of energy transport through this interval is achieved at a source temperature of about 670°R or 372°K.

Natural fog models, at a temperature of 50°F (10°C) have been chosen to represent "light" and "heavy" fog. Two values of volume extinction coefficient, sometimes called optical density, were chosen for illustration in this paper. The optically thinner case of extinction coefficient is taken as 10 km^{-1} and represents a "light" fog with a visibility of approximately the length of a football field. The optically thicker case has an extinction coefficient of 80 km^{-1} and represents a "heavy" fog with a visibility of the order of magnitude of two standard size automobile lengths.

The parameters which might be calculated for comparative purposes are numerous. In this paper the local instantaneous rate of heat transfer per unit volume, based on the initial properties of the aerosol, can be determined by means of an energy balance between the source and the subspaces of the accounting shell. This energy balance is achieved by calculating the rate of energy release from a typical sample of the source, in the appropriate wavelength interval for direct transfer to the droplets, and assigning an equal discrete portion of this energy to each of the characteristic energy bundles released from the source. The number of such energy bundles absorbed in each subspace of the accounting shell has been cataloged during the application of the Monte Carlo method to the analytical model. Each energy bundle represents a rate of energy release and/or energy absorbed. With a homogeneous aerosol regardless of droplet movement, the mass of liquid in each subspace is fixed. Knowledge of the rate of energy absorption can easily be transformed to the time required, at this instantaneous rate and for a homogeneous aerosol, to accumulate sufficient energy to be equal to the latent heat of vaporization for the mass of liquid in a given subspace. Since this time is associated with a number of assumptions which would not hold true in the actual time dependent transfer of energy, it is referred to in this work as the pseudo-evaporation time. Although this pseudo-evaporation time does not give a true picture of the rate of dispersion of a natural fog, it does provide a parameter for comparing the effect of changes in the ratio of absorption coefficient to extinction coefficient and in the type of scattering function used to characterize the homogeneous aerosol.

Standard aerosol model properties, considered reasonable values for natural fog, and common to all illustrated comparisons are represented by the abs/ext ratio of 0·4 and a strong forward scattering function. Figures 3 and 4 depict the spatial locations, in a radial plot, of the lines of equal rate of radiative energy transfer per unit volume (pseudo-evaporation times in parentheses) for extinction coefficients of 10 and 80 km^{-1} respectively. In these illustrations the standard aerosol properties are used.

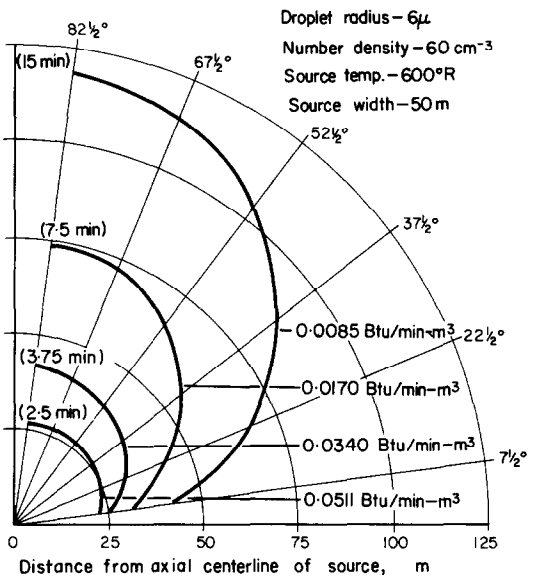

FIG. 3. Locations of equal radiative heat transfer rate per unit volume (equal pseudo-evaporation time) for a long rectangular source. 54997 histories; 25000 absorptions; 36623 scatterings; anisotropic scattering (F); optical density, 10·0 km^{-1}; absorption/extinction, 0·4.

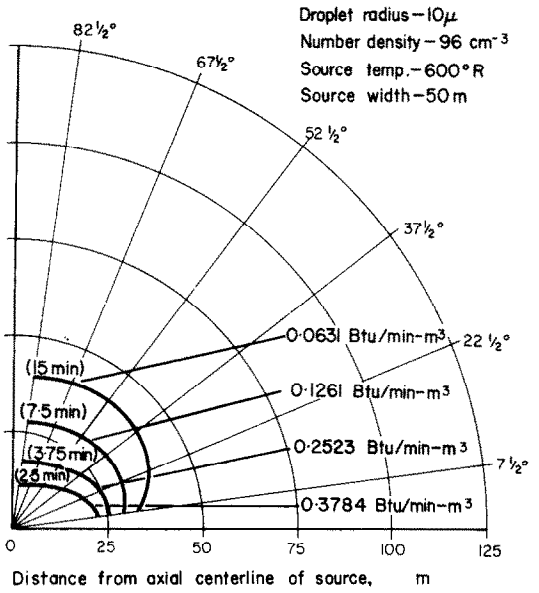

FIG. 4. Locations of equal radiative heat transfer rate per unit volume (equal pseudo-evaporation time) for a long rectangular source. 50921 histories; 50000 absorptions; 74922 scatterings; anisotropic scattering (F); optical density, 80·0 km^{-1}; absorption/extinction, 0·4.

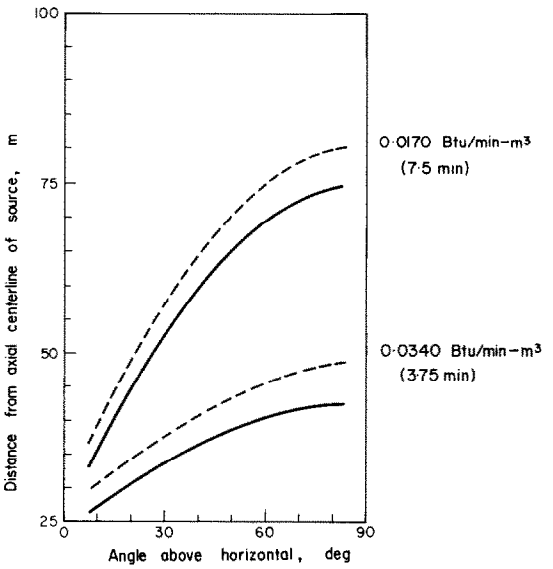

FIG. 5. Comparative locations of lines of equal radiative heat transfer rate per unit volume (equal pseudo-evaporation time). Rectangular source; optical density, 10 km^{-1}; anisotropic scattering (F); mean free path, 100 m; ——— abs/ext, 0·4; - - - - - - abs/ext, 0·5.

Figures 5 and 6 provide a comparative study, illustrated in a rectangular plot to provide good line separation, of the spatial distribution of radiative exchange for two values of the ratio of absorption coefficient to extinction coefficient. The lines depicting equal rate of radiative energy transfer per unit volume (equal pseudo-evaporation time) for the abs/ext ratio of 0·4 are the same as those shown on Figs. 3 and 4 for comparable extinction coefficients with the strong forward scattering function.

Figures 7 and 8 represent the comparison between strong forward anisotropic scattering and isotropic scattering. The ratio of absorption coefficient to extinction coefficient is 0·4 for both figures, and the data for the strong forward scattering aerosol is the same as that found on Figs. 3 and 4 for comparable extinction coefficients.

Insight into the meaning of these comparative illustrations is enhanced by the knowledge that the mean free path of a given energy

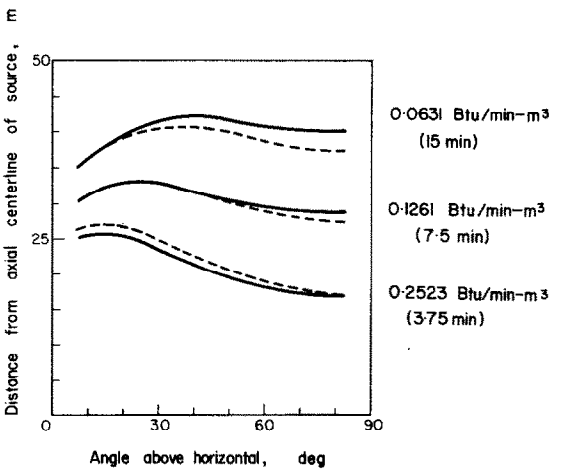

FIG. 6. Comparative locations of lines of equal radiative heat transfer rate per unit volume (equal pseudo-evaporation time). Rectangular source; optical density, 80 km^{-1}; anisotropic scattering (F); mean free path, 12·5 m; ——— abs/ext, 0·4; - - - - - abs/ext, 0·5.

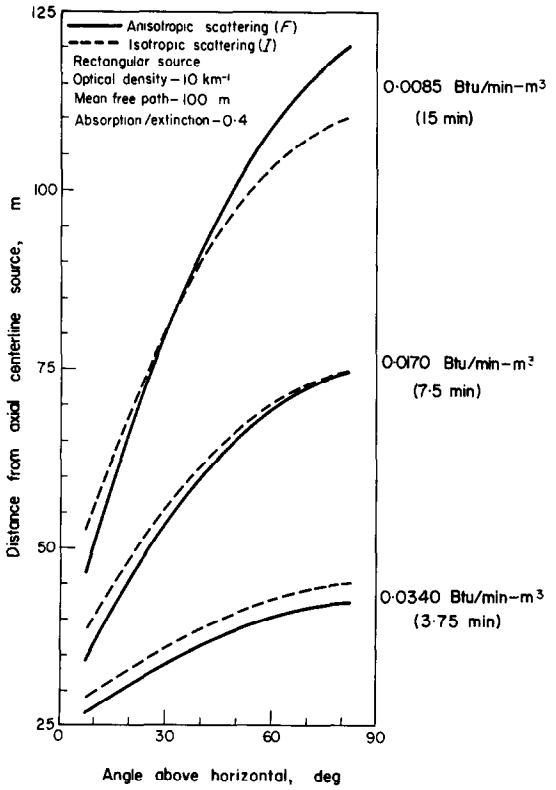

FIG. 7. Comparative locations of lines of equal radiative heat transfer rate per unit volume (equal pseudo-evaporation time).

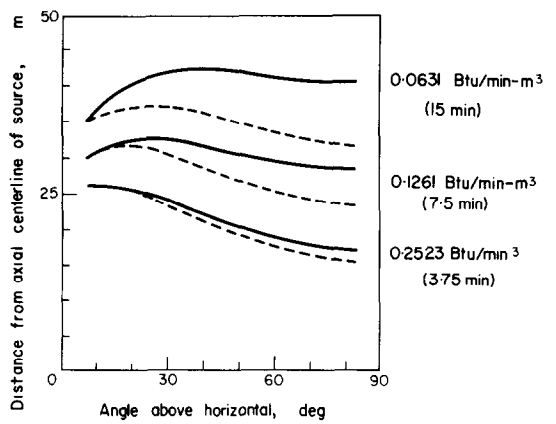

FIG. 8. Comparative locations of lines of equal radiative heat transfer rate per unit volume (equal pseudo-evaporation time). Rectangular source; optical density, 80 km^{-1}; absorption/extinction, 0·4; ——— anisotropic scattering (F); – – – – – isotropic scattering (I).

bundle is equal to the reciprocal of the volume extinction coefficient or optical density. For this reason, the optically thinner cases with long mean free paths show different comparative trends than the optically thicker cases with short mean free paths.

For example, heat transfer to droplets near the source for the optically thinner case is enhanced by the higher abs/ext ratio because a higher percentage of the interactions close to the source are absorptions. However, when the optical density is increased and the mean free path becomes short, this increase in the abs/ext ratio is detrimental to heat transfer at some distance from the source because fewer energy bundles penetrate to distances that exceed the mean free path.

In the case of isotropic scattering, the extinction coefficient of the aerosol again becomes important. In the optically thinner case, the tendency of isotropic scattering to return energy bundles in a backward direction as often as they continue in a forward direction is beneficial to dissipation or evaporation close to the source because escape to extended distances from the source is less likely. On the other hand when the optically thicker case is studied, it becomes important for a large number of energy bundles to penetrate to greater depths into the aerosol in order to effect heat transfer at greater distances from the source. In this instance isotropic scattering is detrimental in comparison to strong forward scattering.

CONCLUSION

Radiative heat transfer from a plane area source to a surrounding aerosol can be determined efficiently by means of a statistical analytical model and application of the Monte Carlo model. Although this paper has concentrated on a particular source–aerosol model, the analytical method is well suited to other models of this general type [26]. The finite nature of the source, as well as the multiple independent scatterings involved, led to the decision to use this analytical method.

Because the long rectangular example source was considered to represent an airport runway, it is not possible to increase the exchange of energy by elevating the source temperature above modest levels compatible with aircraft operations. However, the use of this source as a primary thermal dissipation system, coupled with either additional thermal devices or seeding techniques to provide emergency or temporary assistance in severe cases, could be of some interest. In addition to the contribution made to fog dissipation, the use of a heated runway for drying or for ice and snow removal would represent a related potential benefit.

The numerical data illustrated in the paper indicates the importance of the ratio of absorption coefficient to extinction coefficient on the spatial distribution of radiative energy exchange. Changes in this parameter might be effected by seeding the aerosol with appropriate agents. Isotropic scattering is shown to be a simplifying assumption of doubtful value for this source–aerosol model.

While it would be unrealistic to make explicit statements of the cost of dissipating fog over an airport runway on the basis of this work, the implications of the numerical results reported here are significant. Using an energy cost of 1 cent per kWh and assuming all direct radiative energy transfer to the droplets is converted to evaporation, a comparable opening can be achieved for a cost significantly below that reported for FIDO systems with a "typical" fog under calm conditions [2]. Candor demands that this comparison be considered as indicative of the significance of the radiative transport rather than as a critical evaluation of FIDO systems. Important considerations not included in this work are the actual mechanism of droplet evaporation, the coupled transport due to convection, and the time dependent character of the optical and physical properties of the aerosol. While a cross wind would not affect the rate of radiative energy transfer, it would affect the dissipation of the fog. Mild cross winds, ones which would keep a droplet in a favorable spatial envelope for radiative heat transfer, could be accommodated by this source–aerosol model. The source could be rearranged as strips on either side of the runway to change the shape of the radiative exchange envelope in order to accommodate somewhat larger components of wind normal to the runway. Large scale experiments are indicated as a means for obtaining data from which real-time fog dissipation analysis, using a field of radiation, can become a reasonable goal.

REFERENCES

1. H. G. HOUGHTON and W. H. RADFORD, On the local dissipation of natural fog, *Papers in Physical Oceanography and Meterology*, Massachusetts Institute of Technology and Woods Hole Oceanographic Institution, Vol. VI, No. 3, October (1938).
2. C. S. DOWNIE and R. B. SMITH, Thermal techniques for dissipating fog from aircraft runways, USAF ARCRC-TN-58-477, Geophysics Research Directorate, Air Force Cambridge Research Center, Air Research and Development Command, Bedford, Mass. (1958).
3. G. W. ROBERTSON, Low temperature fog at the Edmonton Airport as influenced by moisture from combustion of natural gas, *Q. J. R. Met. Soc.* **81**, 190–197 (1954).
4. V. I. BELYAEV and I. S. PAVLOVA, On the possibility of influencing the weather by artificial dissipation of cloudiness, *Bull. Acad. Sci. USSR Geophys. Ser.* **1**, 129–133 (1962).
5. R. J. PILIE', W. C. KOCMOND and J. E. JIUSTO, Warm fog suppression in large-scale laboratory experiments, *Science, N.Y.* **157**, 1319–1320 (1967).
6. R. J. PILIE', Investigation of warm fog properties and fog modification concepts, Project Fog Drops, NASA CR-368, Cornell Aeronautical Laboratory, Inc., Buffalo, New York (1966).
7. J. E. JIUSTO, R. J. PILIE' and W. C. KOCMOND, Fog modification with giant hygroscopic nuclei, *J. Appl. Met.* 7, 860–869 (1968).
8. W. L. WOLFE (editor), *Handbook of Military Infrared Technology*. U.S. Government Printing Office, Washington DC (1965).
9. H. G. HOUGHTON, The size and size distribution of fog particles, *Physics* **2**, 467–475 (1932).
10. A. C. BEST, Drop-size distribution in cloud and fog, *Q. J. R. Met. Soc.* **77**, 418–426 (1951).
11. W. E. K. MIDDLETON, *Vision through the Atmosphere*. University of Toronto Press, Toronto (1952).
12. A. J. ARNULF, J. BRICARD, E. CURE and C. VERET, Transmission by haze and fog in the spectral region 0·35–10 μ, *J. Opt. Soc. Am.* **47**, (6) 491–498 (1957).
13. J. C. JOHNSON and J. R. TERRELL, Transmission cross sections for water spheres illuminated by infrared radiation, *J. Opt. Soc. Am.* **45**, (6) 451–454 (1955).
14. D. DEIRMENDJIAN, *Electromagnetic Scattering* (edited by M. KERKER). Macmillan, New York (1963).

15. E. M. FEIGELSON, *A Collection of Articles on Dynamic Meterology* (edited by I. A. KIBEL) pp. 73–104. American Geophysical Union, Consultants Bureau, New York (1960).
16. R. PENNDORF, Research on aerosol scattering in the infrared, Scientific report No. 2, Mie scattering in the forward area, USAF Geophysics Research Directorate, Air Force Cambridge Research Center, Air Research and Development Command, RAD-TR-60-10, Bedford, Mass. (1960).
17. B. S. PRITCHARD and W. G. ELLIOTT, Two instruments for atmospheric optics measurements, *J. Opt. Soc. Am.* **50**, 191–202 (1960).
18. E. PARZEN, *Modern Probability Theory and Its Applications*. John Wiley, New York (1960).
19. J. R. HOWELL and M. PERLMUTTER, Monte Carlo solution of thermal transfer through radiant media between gray walls, *Trans. Am. Chem. Soc. Mech. Engrs* **86**, 116–122 (1964).
20. M. PERLMUTTER and J. R. HOWELL, Radiant transfer from gray gas between concentric cylinders using Monte Carlo, *J. Heat Transfer* **86**, 169–179 (1964).
21. L. W. STOCKHAM, Radiative heat transfer from a finite cylindrical particle cloud, Ph.D. Dissertation, University of Oklahoma (1967).
22. P. M. CAMPBELL, Monte Carlo method for radiative transfer, *Int. J. Heat Mass Transfer* **10**, 519–527 (1967).
23. G. J. MULLANEY, W. H. CHRISTIANSEN and D. A. RUSSELL, Fog dissipation using a CO_2 laser, *Appl. Phys. Lett.* **13**, 145–147, 15 August (1968).
24. T. J. LOVE, *Radiative Heat Transfer*. Charles Merrill, Columbus, Ohio (1968).
25. E. M. SPARROW and R. D. CESS, *Radiation Heat Transfer*. Brooks/Cole, Belmont, California (1966).
26. G. L. SCOFIELD, Radiative heat transfer from an arbitrary plane source to a semi-infinite aerosol, Ph.D. Dissertation, University of Oklahoma (1968).

ANALYSE DU TRANSPORT DE CHALEUR PAR RAYONNEMENT VERS DU BROUILLARD A PARTIR D'UNE PISTE CHAUFFEE D'AEROPORT

Résumé—Le transport de chaleur par rayonnement entre une source plane et un aérosol est étudié à l'aide de la méthode de Monte Carlo. L'énergie thermique est transportée à partir d'une longue source rectangulaire à des modèles de brouillards naturels monodispersés. L'analyse est seulement valable pour le transport par rayonnement et ne comprend pas la convection qui serait couplée dans une analyse complète. Le transport direct d'énergie aux gouttelettes de l'aérosol est étudié pour des valeurs du coefficient d'extinction de 10 km^{-1} et 80 km^{-1}, des rapports du coefficient d'absorption au coefficient d'extinction de 0,4 et 0,5, et des fonctions de dispersion du type fort vers l'avant et isotropes. Un rayonnement monochromatique à une longueur d'onde de 10 microns est employé et l'on tient compte de multiples diffusions indépendantes.

Les résultats numériques sont illustrés d'une manière qui exprime la distribution spatiale des interactions de rayonnement et expose l'implication du mode d'échange d'énergie comme moyen de disperser le brouillard sur les pistes d'aéroport.

ANALYSE DES WÄRMEÜBERGANGES DURCH STRAHLUNG VON EINER BEHEIZTEN FLUGHAFENPISTE AN NEBEL.

Zusammenfassung—Der Strahlungswärmetransport zwischen einer ebenen Fläche und einem Aerosol wird nach der Monte Carlo Methode untersucht. Die Wärmeenergie wird von einer langen rechteckigen Fläche an Modelle für einfach streuenden, natürlichen Nebel übertragen. Die Berechnung gilt nur für den Wärmetransport durch Strahlung und schliesst die Konvektion, die bei einer vollständigen Berechnung mit der Strahlung gekoppelt wäre, nicht mit ein. Der direkte Wärmetransport an die Tropfen des Nebels wird berechnet für Werte des Extinktionskoeffizienten von 10 km^{-1} und 80 km^{-1}, für Verhältnisse des Absorptionskoeffizienten zum Extinktionskoeffizienten von 0,4 und 0,5 und für Streufunktionen des direkten, isotropen Typs. Monochromatische Strahlung der Wellenlänge 10 μm wird verwendet, mehrfache unabhängige Streuung wird berücksichtigt. Die numerischen Ergebnisse werden so dargestellt, dass die räumliche Verteilung der Wirking der Strahlung zum Ausdruck kommt und dass Folgerungen hinsichtlich dieser Art des Wärmeaustausches als Mittel für die Nebelauflösung über Flughafenposten gezogen werden können.

ЛУЧИСТЫЙ ПЕРЕНОС ТЕПЛА ОТ НАГРЕТОЙ ВЗЛЕТНО-ПОСАДОЧНОЙ ДОРОЖКИ К ТУМАНУ

Аннотация—Методом Монте-Карло исследуется лучистый теплообмен между плоским источником и аэрозолем. Тепловая энергия переносится от длинного прямоугольного источника к монодисперсным естетственным модельным средам тумана. Вычисляется только лучистый перенос и не учитывается конвекция. Полный анализ должен включать в себя как лучистый перенос, так и конвекцию. Исследуется непосредственный перенос энергии к каплям аэрозоля при значениях коэффициента затухания от 10 км$^{-1}$ до 80 км$^{-1}$, при отношениях коэффициентов поглощения и затухания 0,4 и 0,5 и для функций рассеяния изотропного типа. Используется монохроматическое излучение на длине волны (10 μ); приводится многократное независимое рассеяние. Иллюстрируются численные результаты, которые отражают пространственное распределение лучистых взаимодействий и показывают, что энергообмен можно использовать для рассеяния тумана на взлетно-посадочных дорожках.